

1 **LIMS observations of lower stratospheric ozone in the southern polar springtime of 1978**

2
3 Ellis Remsberg¹, V. Lynn Harvey², Arlin Krueger³, Larry Gordley⁴,
4 John C. Gille⁵, and James M. Russell III⁶

5
6 ¹Science Directorate, NASA Langley Research Center, 21 Langley Blvd, Mail Stop 401B,
7 Hampton, VA 23681, USA

8 ²Laboratory for Atmospheric and Space Physics, University of Colorado Boulder, 3665
9 Discovery Drive, Boulder, CO 80303, USA

10 ³Emeritus Senior Scientist, Code 614 Atmospheric Chemistry and Dynamics Laboratory, NASA
11 Goddard Space Flight Center, Greenbelt, MD 20771, USA

12 ⁴GATS, Inc., 11864 Canon Blvd., Suite 101, Newport News, VA 23606, USA

13 ⁵Senior Scientist Emeritus, National Center for Atmospheric Research, P.O. Box 3000, Boulder,
14 CO 80307-3000, USA

15 ⁶Endowed Professor and Co-Director, Center for Atmospheric Sciences, Hampton University,
16 Hampton, VA 23668, USA

17
18
19
20 Correspondence to: Ellis Remsberg (ellis.e.remsberg@nasa.gov)

21
22 For submission to Atmospheric Chemistry and Physics Journal

23 February, 2020

24 **Abstract**

25 The Nimbus 7 limb infrared monitor of the stratosphere (LIMS) instrument operated from
26 October 25, 1978, through May 28, 1979. This note focuses on its Version (V6) data and
27 indications of ozone loss in the lower stratosphere of the southern hemisphere, subpolar region
28 during the last week of October 1978. We provide profiles and maps that show V6 ozone values
29 of only 2 to 3 ppmv at 46 hPa within the edge of the polar vortex near 60°S from late October
30 through mid-November 1978. There are also low values of V6 nitric acid (~3 to 6 ppbv) and
31 nitrogen dioxide (<1 ppbv) at the same locations, indicating that conditions were suitable for a
32 chemical loss of Antarctic ozone some weeks earlier. These “first light” LIMS observations
33 provide the earliest, space-based view of conditions within the lower stratospheric ozone layer of
34 the southern polar region in springtime.

35

36 **1 Introduction and historical context**

37 The Nimbus 7 Total Ozone Mapping Spectrometer (TOMS) provided the first daily image of
38 total ozone for the Southern Hemisphere (SH) on November 1, 1978. That image in Figure 1
39 shows an equatorward extension of the region of low polar, total column ozone (TCO) between
40 90°E and 135°E. Minimum TCO is of the order of 270 Dobson units (DU) at (75°S, 90°E) on
41 this day. As a comparison, Farman et al. (1985) reported ground-based measurements of total
42 ozone of about 225 DU on November 1 for 1980-1984 at Halley Bay (76°S, 333°E) and of about
43 270 DU at Argentine Islands (65°S, 296°E) (see also TOMS total ozone values of Table 2 in
44 Stolarski et al. (1986)). We note, however, that those values are higher than 220 DU, “definition
45 of the threshold for ozone hole conditions” (WMO, 2018).

46

47 There are very few observations of lower stratospheric ozone above Antarctica prior to
48 November 1978, especially for the months of September and October when the seasonal loss of
49 ozone is most significant (WMO, 2018). The historic Nimbus 7 Limb Infrared Monitor of the
50 Stratosphere (LIMS) experiment (Gille and Russell, 1984) provided data for middle atmosphere
51 temperature, geopotential height (GPH), ozone, water vapor (H₂O), nitric acid vapor (HNO₃),
52 and nitrogen dioxide (NO₂) from October 25, 1978, through May 28, 1979, for scientific analysis

53 and for comparisons with atmospheric models (e.g., Langematz et al., 2016). Remsberg et al.
54 (2007) provide a description of its Version 6 (V6) ozone profiles. The mapping of the V6
55 profiles to the LIMS Level 3 product employs a sequential estimation algorithm with a relaxation
56 time of about 2.5 days for analyses of its zonal, 6-wavenumber Fourier coefficients at each of 28
57 pressure levels of the middle atmosphere (Remsberg and Lingenfelter, 2010). We then
58 generated daily, polar stereographic plots of V6 ozone and HNO₃ on pressure surfaces based on a
59 gridding (2° latitude and 5.625° longitude) from those coefficients.

60

61 This note focuses on the character of the polar vortex and of the V6 ozone, HNO₃, and NO₂ in
62 that region of the lower stratosphere during the last week of October 1978. The LIMS
63 measurements extend to only 64°S, due to the orbital inclination of Nimbus 7 and to the viewing
64 geometry of the LIMS instrument (Gille and Russell, 1984). We will show that the profiles and
65 pressure surface maps indicate that there was a loss of SH polar ozone during the springtime.
66 Section 2 contains plots that show a loss of ozone inside the vortex in late October. Section 3
67 reports on evidence for a denitrification of the air in the same region, indicating that there was a
68 chemical loss of ozone some weeks earlier. Section 3 also presents time versus longitude or
69 Hovmöller diagrams that reveal good correspondence for the low ozone and HNO₃ values within
70 the vortex region well into November. Section 4 summarizes the findings.

71

72 **2 Antarctic ozone from late October to early November 1978**

73 Figure 2 shows SH polar plots of V6 ozone mixing ratios at 46.4 hPa for October 26 and for
74 November 1, where the orbital measurements of LIMS extend only to 64°S. The plot at right
75 shows that there are minimum ozone values of about 2.6 ppmv near 120°E and 315°E at 60°S on
76 November 1, which agrees reasonably with the locations of low total ozone from the TOMS
77 image of Fig. 1. Ozone is of order 3.5 to 4 ppmv at most other longitudes. Low ozone occurs
78 within the edges of the polar vortex, based on the concurrent GPH field from the operational
79 ECMWF Re-Analysis or ERA-40 products (Uppala et al., 2005). The bold contour in Fig. 2
80 denotes the edge of the vortex, in the manner of Harvey et al. (2002). We define the vortex edge
81 as the streamfunction contour coincident with maximum wind speed that also encloses a region

82 of rotation. Meek et al. (2017) showed that this definition of the vortex edge is in good
83 agreement with the PV-gradient based definition of Nash et al. (1996). We note that daily plots
84 of GPH are also available from LIMS V6. However, they exhibit a discontinuous anomaly at the
85 46-hPa level for the vortex region between October 29 and 31, due to an interpolation of
86 National Meteorological Center (NMC) GPH analyses supplied to the Nimbus 7 Project and used
87 for the baseline pressure level of 50 hPa for the V6 GPH product (Remsberg et al., 2004). V6
88 geometric height and GPH profiles above and below that level are the result of a hydrostatic
89 integration of the LIMS-retrieved temperature versus pressure profiles of $T(p)$. Maps of V6
90 GPS farther away from the 50-hPa level are very similar to those from ERA-40.

91

92 LIMS began its daily observations one week earlier than TOMS or on October 25, and the left
93 plot of Fig. 2 shows that the ozone for October 26 at 31°E is about half of that at 119°E on
94 November 1. The vortex on October 26 extends toward lower latitudes from about 60°S, 40°E.
95 Both the vortex and region of low ozone deform and undergo a clockwise rotation from October
96 26 onward, such that their low values extend equatorward at 120°E and at 315°E on November
97 1. Bodeker et al. (2002) reported that the edge of the vortex often extends to near 60°S during
98 October, and Stolarski et al (1986, their Fig. 1) and Hassler et al. (2011) reported on an
99 analogous clockwise rotation of the vortex during October.

100

101 **3 Findings of denitrification of the vortex air in late October**

102 The location of the vortex edge is helpful in deciding which V6 species profiles one ought to
103 examine with regard to any constraints from HNO_3 and NO_2 on the ozone chemistry. As an
104 example, Fig. 3 shows V6 Level 2 ozone profile segments from 11.4 to 88 hPa for two locations
105 on October 26, where ozone is now presented in units of partial pressure (in mPa) for a better
106 delineation of its relative changes in the subpolar lower stratosphere. Estimates of accuracy for
107 single V6 ozone profiles are 14%, 26%, and 34% for 10 hPa, 50 hPa, and 100 hPa, respectively
108 (see row (g) of Table 1 in Remsberg et al., 2007). The V6 ozone profile (black solid) at 54.9°S,
109 119°E is just outside the October 26 vortex, as shown by the black dot in Fig. 2, and its ozone
110 values are nominal for subpolar latitudes. The largest contribution to total ozone from that

111 profile in Fig. 3 occurs at the 68-hPa level. A second V6 ozone profile (solid red) is from
112 59.5S°, 31°E, and it is in a region of lower GPH as shown by the red dot in Fig. 2. Its ozone
113 decreases rapidly from ~8.0 mPa at the 53-hPa level to 2.6 mPa at the 88-hPa level, indicating a
114 significant loss of ozone in the lower stratosphere sometime prior to October 26. Komhyr et al.
115 (1988, their Fig. 10) and Gernandt (1987) show from ozonesonde measurements that most of the
116 observed losses of ozone for the mid-1980s occurred in the vortex in September and early
117 October. Therefore, we also include in Fig. 3 an ozonesonde profile (solid green) from Syowa
118 station (69°S, 40°E—the green dot in Fig. 2) for September 3, 1978, perhaps before there were
119 any pronounced losses of ozone. Its ozone profile values are intermediate of those for the two
120 V6 profiles of October 26.

121
122 Loss of ozone due to reactive chlorine chemistry proceeds effectively in the presence of air that
123 has undergone denitrification (Solomon, 1999; Müller et al., 2008). Lambert et al. (2016)
124 somewhat loosely set an HNO₃ threshold of < 5 ppbv for indicating denitrification at 46 hPa,
125 based on Microwave Limb Sounder (MLS) data of 2008. Nitrous oxide is the source molecule
126 for odd nitrogen (mainly HNO₃) in the lower stratosphere, and its tropospheric values have
127 grown by only a small amount from 1975 (~296 ppbv) through 2008 (~322 ppbv) (WMO, 2018);
128 the HNO₃ threshold of 5 ppbv should also be representative for 1978. Thus, in Figure 3 we also
129 show the accompanying V6 profiles of HNO₃ and nighttime NO₂ for the same two locations on
130 October 26. HNO₃ and NO₂ at 31°E are a half (or 3 ppbv) and a third (or < 1 ppbv),
131 respectively, of those at 119°E below about the 31-hPa level. Thus, both species indicate that
132 there was a denitrification of the air in the vortex region and a likely loss of ozone due to reactive
133 chlorine chemistry in the presence of polar stratospheric clouds (PSCs) several weeks earlier
134 (Solomon, 1999; WMO, 2018). Although the V6 temperature at 31°E on October 26 was 206 K
135 (at 53 hPa), it is normal to find temperatures in the Antarctic vortex that are below the chlorine
136 activation threshold value of 195 K and in the presence of PSCs during September and early
137 October (WMO, 2018).

138
139 Figure 4 shows the corresponding V6 plots of HNO₃ at 46 hPa in terms of its mixing ratios,
140 which have an estimated accuracy of ~9% (Remsberg et al., 2010, Table 10). There are very low

141 values of HNO_3 on October 26 poleward of 60°S and from 31°E to at least 90°E , indicating an
142 earlier conversion of HNO_3 from vapor to condensed phase and the sedimentation of larger
143 HNO_3 containing particles rather than an advection of low HNO_3 from lower latitudes. Low
144 HNO_3 mixing ratios are also present within the vortex region on November 1. Analogous polar
145 plots of the nighttime NO_2 fields are quite noisy (not shown) due to the large uncertainties for
146 tangent layer NO_2 in the lower stratosphere. Nevertheless, most of the odd nitrogen reservoir at
147 46 hPa comes from HNO_3 , not NO_2 . Together, they indicate the extent of denitrification of the
148 air in the vortex region during late October 1978.

149
150 We show in Figs. 5 and 6 the details of the changing ozone and nitric acid from late October
151 through November. Figure 5 displays time/longitude or Hovmöller diagrams for both species at
152 60°S ; thick black contours indicate the vortex edge and dotted horizontal lines the vortex
153 interior. The occurrence of lowest species mixing ratios shows clearly in the vortex region in
154 late October. Figure 6 extends the findings of Fig. 5 through the end of November, and there is
155 an eastward progression of the region of low values from late October to early November.
156 Reduced mixing ratios of those species occur inside the vortex until about November 25, as
157 expected for chemicals that are tracers of air motions in the lower stratosphere. The vortex
158 distorts and then exhibits a stationary wave-1 pattern from November 5 onward, where height is
159 lowest near 0°E . Mixing of air across the vortex edge appears slow for both ozone and HNO_3
160 during that time.

161

162 **4 Summary and concluding remarks**

163 We find low V6 ozone mixing ratios of order 2 to 3 ppmv at 60°S within the edge of the polar
164 vortex at 46 hPa during the last week of October and well into November 1978. There is good
165 agreement between the V6 ozone map at 46 hPa and the TOMS image of total ozone in the
166 region of the vortex on November 1. Low V6 HNO_3 mixing ratios of order 3 to 6 ppbv at the
167 same locations indicate denitrification and conditions that were suitable for a chemical loss of
168 Antarctic ozone some weeks earlier. We note that equivalent effective stratospheric chlorine
169 (EESC) value of 2.01 ppbv used to predict conditions for the depletion of ozone in 1980 is about

170 twice that of 1950, while the 1980 value is only half that of 2000 (Newman et al., 2007). In
171 hindsight and based on the LIMS V6 dataset, we conclude that there was very likely some
172 halogen-catalyzed loss of ozone in the southern polar vortex in winter/spring of 1978. Yet, those
173 ozone losses in the SH spring were not to the low level of a true “ozone hole” (<220 DU total
174 ozone). We also conclude that the LIMS V6 Level 2 profiles and the daily-analyzed maps from
175 their Level 3 zonal coefficients represent useful comparison data for simulations of the expected
176 changes in Antarctic ozone in spring 1978.

177

178 **Data Availability**

179 The LIMS V6 data archive is at the NASA EARTHDATA site of EOSDIS and its website:
180 <https://search.earthdata.nasa.gov/search?q=LIMS>). Nimbus 7 TOMS ozone is at
181 https://disc.gsfc.nasa.gov/datacollection/TOMSN7L2_008.html. ECC ozonesonde ozone
182 profiles are available from the World Ozone and Ultraviolet Radiation Data Centre or WOUDC
183 at <https://woudc.org/data/explore.php>. ECMWF Re-Analysis (ERA-40) data are accessible
184 through <https://climatedataguide.ucar.edu/climate-data/era40>.

185

186 *Author Contributions.* ER and VLH wrote the manuscript and prepared the figures with input
187 from all the other co-authors. AK provided information about the TOMS ozone images. LG led
188 the development of the LIMS version 6 algorithms. JCG and JMR are the Co-Principal
189 Investigators of the LIMS experiment. They also commented on the new insight from the
190 findings about ozone and nitric acid of October 1978.

191

192 *Acknowledgements.* VLH acknowledges support from NASA LWS grant NNX14AH54G,
193 NASA HGI grant NNX17AB80G, and NASA HSR grant 80NSSC18K1046. EER carried out
194 his work while serving as a Distinguished Research Associate within the Science Directorate at
195 NASA Langley.

196

197 **References**

198 Bodeker, G. E., Struthers, H., and Connor, B. J.: Dynamical containment of Antarctic ozone
199 depletion, *Geophys. Res. Lett.*, 29, 2-1 to 2-4, <https://doi.org/10.1029/2001GL014206>, 2002.

200

201 Farman, J. C., Gardiner, B. G., and Shanklin, J. D.: Large losses of total ozone in Antarctica
202 reveal seasonal ClOx/NOx interaction, *Nature*, 315, 207-210,
203 <https://www.nature.com/articles/315207a0.risNature>, 1985.

204

205 Gernandt, H.: The vertical ozone distribution above the GDR research base, Antarctica in 1985,
206 *Geophys. Res. Lett.*, 14, 84-66, 1987.

207

208 Gille, J. C. and Russell III, J. M.: The limb infrared monitor of the stratosphere: experiment
209 description, performance, and results, *J. Geophys. Res.*, 84, 5125-5140,
210 <https://doi.org/10.1029/JD089iD04p05125>, 1984.

211

212 Harvey, V.L., Pierce, R. B., Fairlie, T. D., and Hitchman, M. H.: A climatology of stratospheric
213 polar vortices and anticyclones, *J. Geophys. Res.*, 107(D20), 4442,
214 <https://doi.org/10.1029/2001JD001471>, 2002.

215

216 Hassler, B., Bodeker, G. E., Solomon, S., and Young, P. J.: Changes in the polar vortex: effects
217 on Antarctic total ozone observations at various stations, *Geophys. Res. Lett.*, 38, L01805,
218 doi:10.1029/2010GL045542, 2001.

219

220 Komhyr, W. D., Oltmans, S. J., and Grass, R. D.: Atmospheric ozone at South Pole, Antarctica,
221 in 1986, *J. Geophys. Res.*, 93, 5167-5184, <https://doi.org/10.1029/JD093iD05p05167>, 1988.

222

223 Lambert, A., Santee, M. L., and Livesey, N. J.: Interannual variations of early winter Antarctic
224 polar stratospheric cloud formation and nitric acid observed by CALIOP and MLS, *Atmos.*
225 *Chem. Phys.*, 16, 15219-15246, <https://doi.org/10.5194/acp-16-15219-2016>, 2016.

226

227 Langematz, U., Schmidt, F., Kunze, M., Bodeker, G. E., and Braesicke, P.: Antarctic ozone
228 depletion between 1960 and 1980 in observations and chemistry-climate model simulations,
229 *Atmos. Chem. Phys.*, 16, 15619-15627, <https://doi:10.5194/acp-16-15619-2016>, 2016.

230

231 Meek, C. E., Manson, A. H., and Drummond, J. R.: Comparison of Aura MLS stratospheric
232 chemical gradients with north polar vortex edges calculated by two methods, *Adv. Space Res.*,
233 60, 1898-1904, <http://dx.doi.org/10.1016/j.asr.2017-06.009>, 2017.

234

235 Müller, R., Grooß, J.-U., Lemmon, C., Heinze, D., Dameris, M., and Bodeker, G.: Simple
236 measures of ozone depletion in the polar stratosphere, *Atmos. Chem. Phys.*, 8, 251-264, 2008.

237

238 Nash, E. R., Newman, P. A., Rosenfield, J. E., and Schoeberl, M. R.: An objective determination
239 of the polar vortex using Ertel's potential vorticity, *J. Geophys. Res.*, 101, 9471-9478, 1996.

240

241 Newman, P. A., Daniel, J. S., Waugh, D. W., and Nash, E. R.: A new formulation of equivalent
242 effective stratospheric chlorine (EESC), *Atmos. Chem. Phys.*, 7, 4537-4552, 2007.

243

244 Remsberg, E., and Lingenfelter, G.: LIMS Version 6 Level 3 dataset, NASA-TM-2010-216690,
245 available at <http://www.sti.nasa.gov> (last access: 17 September 2019), 13 pp., 2010.

246

247 Remsberg, E. E., Gordley, L. L., Marshall, B. T., Thompson, R. E., Burton, J., Bhatt, P., Harvey,
248 V. L., Lingenfelter, G., and Natarajan, M.: The Nimbus 7 LIMS version 6 radiance conditioning

249 and temperature retrieval methods and results, *J. Quant. Spectros. Rad. Transf.*, 86, 395-424,
250 doi:10.1016/j.jqsrt.2003.12.007, 2004.

251

252 Remsberg, E., Lingenfelter, G., Natarajan, M., Gordley, L., Marshall, B. T., and Thompson, E.:
253 On the quality of the Nimbus 7 LIMS version 6 ozone for studies of the middle atmosphere, *J.*
254 *Quant. Spectros. Rad. Transf.*, 105, 492-518, doi:10.1016/j.jqsrt.2006.12.005, 2007.

255

256 Remsberg, E., Natarajan, M., Marshall, B. T., Gordley, L. L., Thompson, R. E., and
257 Lingenfelter, G. L.: Improvements in the profiles and distributions of nitric acid and nitrogen
258 dioxide with the LIMS version 6 dataset, *Atmos. Chem. Phys.*, 10, 4741-4756,
259 <https://doi.org/10.5194/acp-10-4741-2010>, 2010.

260

261 Solomon, S.: Stratospheric ozone depletion: a review of concepts and history, *Rev. Geophys.*, 37,
262 275-316, <https://doi.org/10.1029/1999RG900008>, 1999.

263

264 Stolarski, R. S., Krueger, A. J., Schoeberl, M. R., McPeters, R. D., Newman, P. A., and Alpert, J.
265 C.: Nimbus 7 satellite measurements of the springtime Antarctic ozone decrease, *Nature*, 322,
266 808-811, <https://doi.org/10.1038/322808a0>, 1986.

267

268 Uppala, S. M., KÅllberg, P. W., Simmons, A. J., Andrae, U., Da Costa Bechtold, V., Fiorino,
269 M., Gibson, J. K., Haseler, J., Hernandez, A., Kelly, G. A., Li, X., Onogi, K., Saarinen, S.,
270 Sokka, N., Allan, R. P., Andersson, E., Arpe, K., Balmaseda, M. A., Beljaars, A. C. M., Van De
271 Berg, L., Bidlot, J., Bormann, N., Caires, S., Chevallier, F., Dethof, A., Dragosavac, M., Fisher,
272 M., Fuentes, M., Hagemann, S., Hólm, E., Hoskins, B. J., Isaksen, L., Janssen, P. A. E. M.,
273 Jenne, R., McNally, A. P., Mahfouf, J.-F., Morcrette, J.-J., Rayner, N. A., Saunders, R. W.,
274 Simon, P., Sterl, A., Trenberth, K. E., Untch, A., Vasiljevic, D., Viterbo, P., and Woollen, J.: The

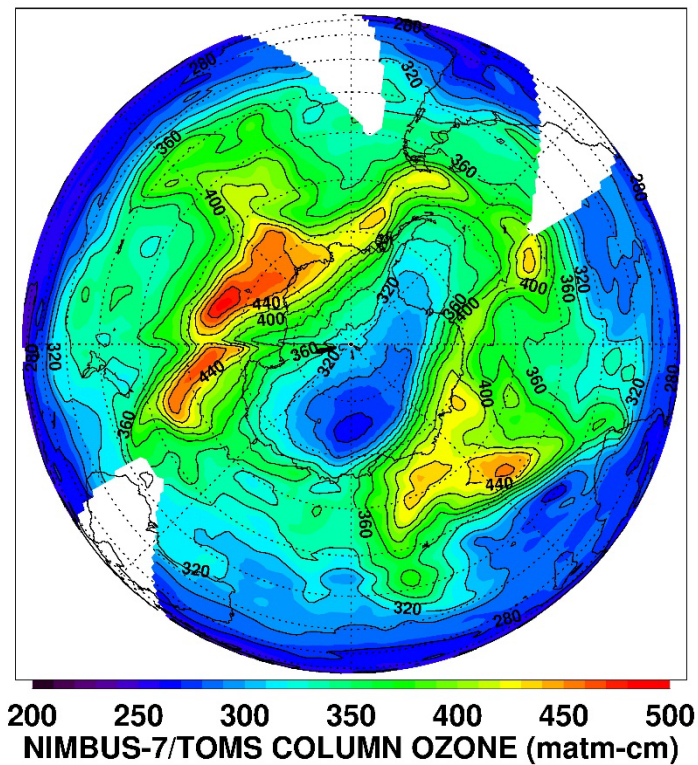
275 ERA-40 reanalysis, Q. J. Roy. Meteorol. Soc., 131, 2961–3012,
276 <https://doi.org/10.1256/qj.04.176>, 2005.

277

278 WMO (World Meteorological Organization), *Scientific Assessment of Ozone Depletion: 2018*,
279 Global Ozone Research and Monitoring Project — Report No. 58, 588 pp., Geneva, Switzerland,
280 2018.

281

282



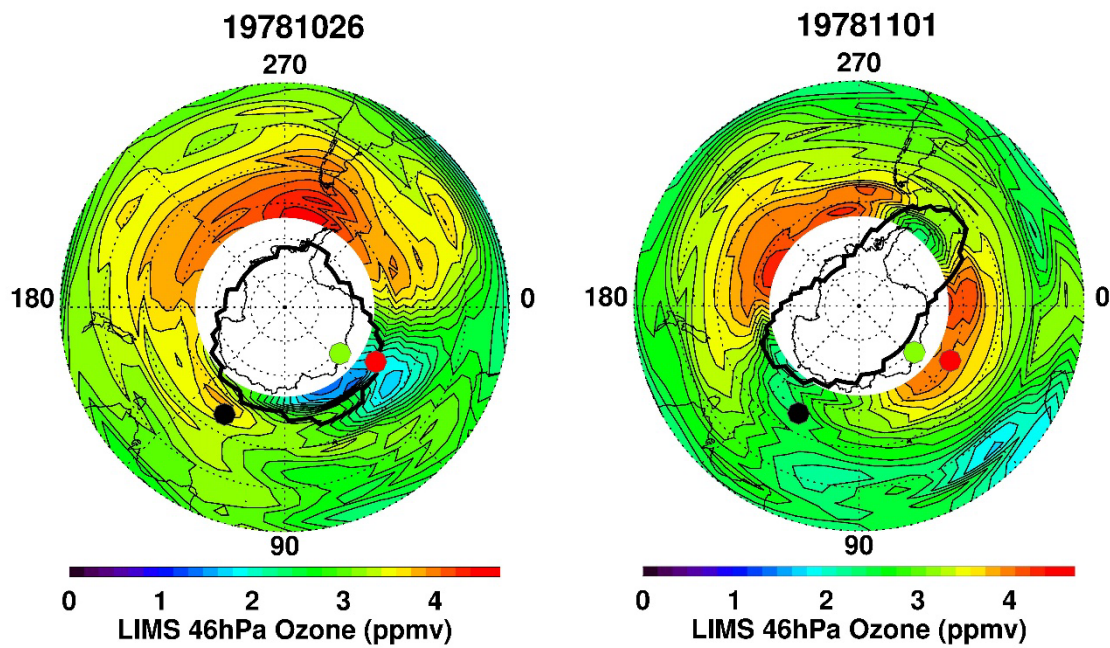
283

284

285 Figure 1—Southern Hemisphere image of total column ozone (TCO) from TOMS for November
286 1, 1978. Longitude orientation is 0°E to the right and 90°E at the bottom; latitude circles
287 (dotted) have a spacing of 10 degrees. White areas indicate where there are discrete data voids
288 or no measurements. Ozone units of matm-cm are equivalent to Dobson units (DU), where 1 DU
289 is 2.687×10^{20} molecules- m^{-2} . Black contours are TCO at intervals of 20 matm-cm.

290

291

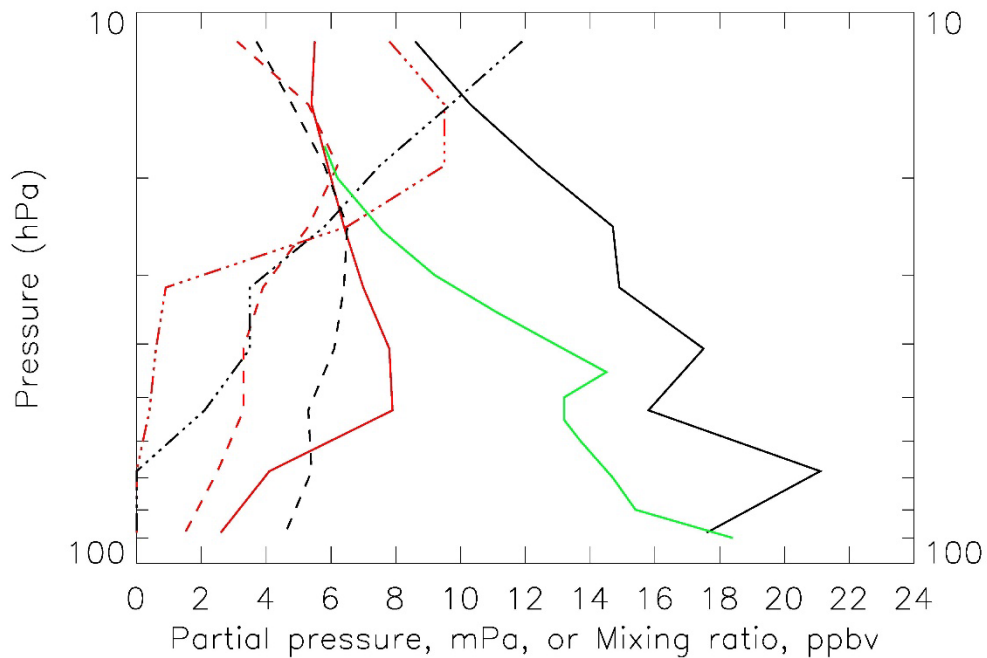


292

293 Figure 2—V6 ozone mixing ratios at 46.4 hPa for October 26 and November 1, 1978. Polar
294 plots extend from 30°S to the Pole and longitude is in °E with 0° at right. Bold contours denote
295 the vortex edge from ERA-40. The superposed, three colored dots correspond to the locations of
296 profiles on October 26 (black and red) and on September 3 (green) in Fig. 3.

297

298

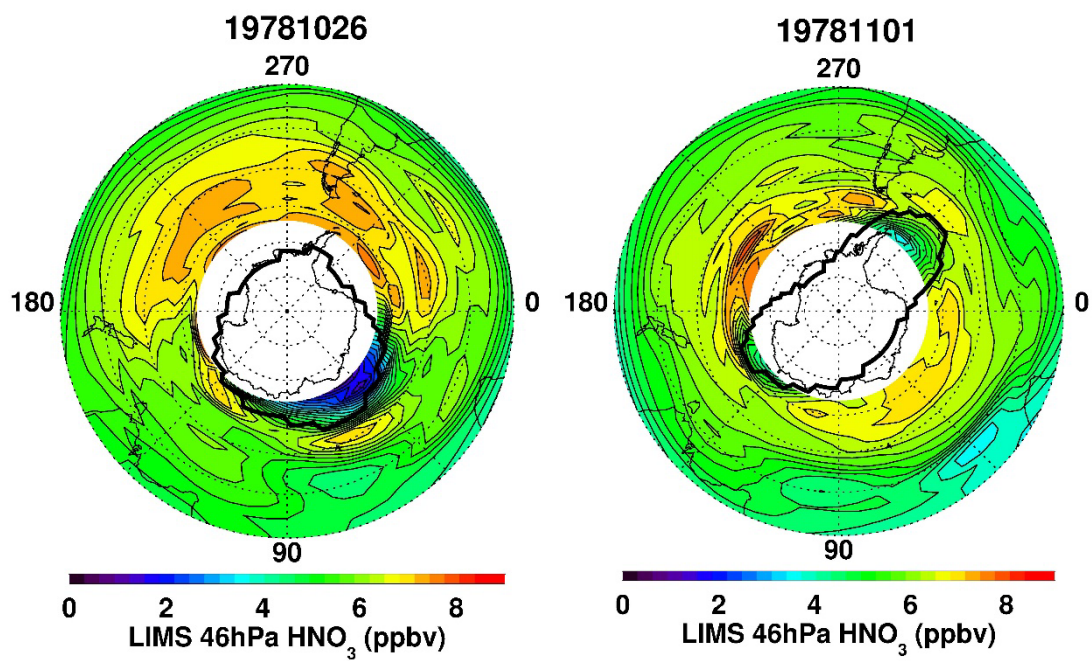


300

301 Figure 3—V6 Level 2 species profiles for 59.5°S, 31°E (red) and 54.9°S, 119.4°E (black) on
 302 October 26, 1978, and from an ozonesonde at Syowa (69°S, 40°E—green) on September 3,
 303 1978. Ozone (solid) has units of millipascals (mPa), while HNO₃ (dashed) and NO₂ (dot-dashed)
 304 have units of ppbv.

305

306

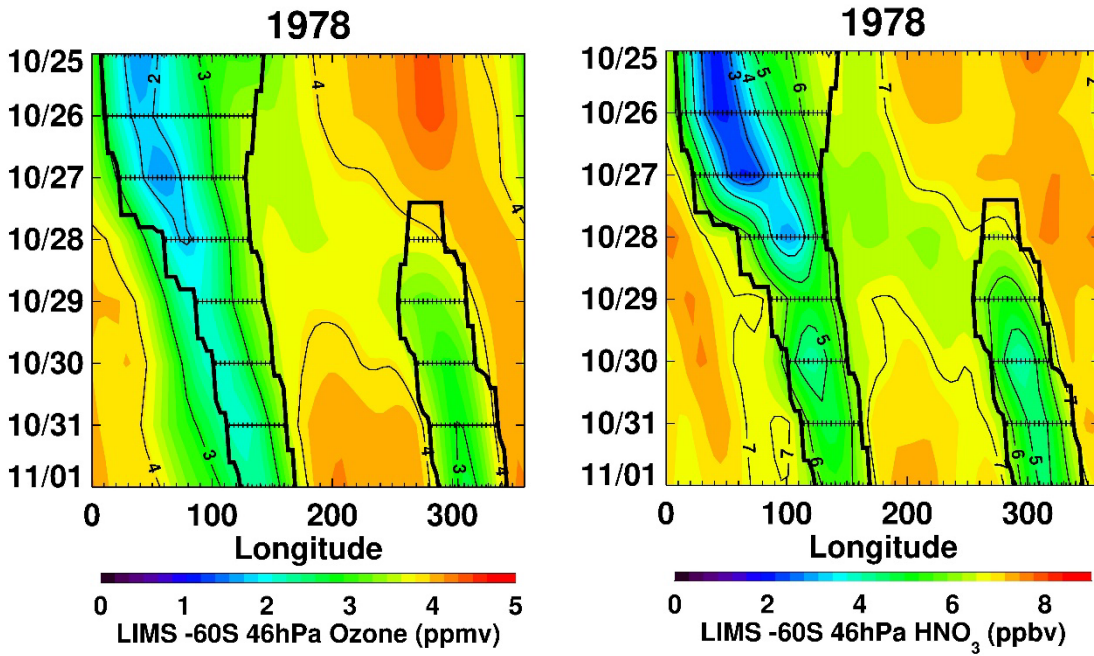


307

308 Figure 4—As in Fig. 2, but for V6 HNO₃.

309

310

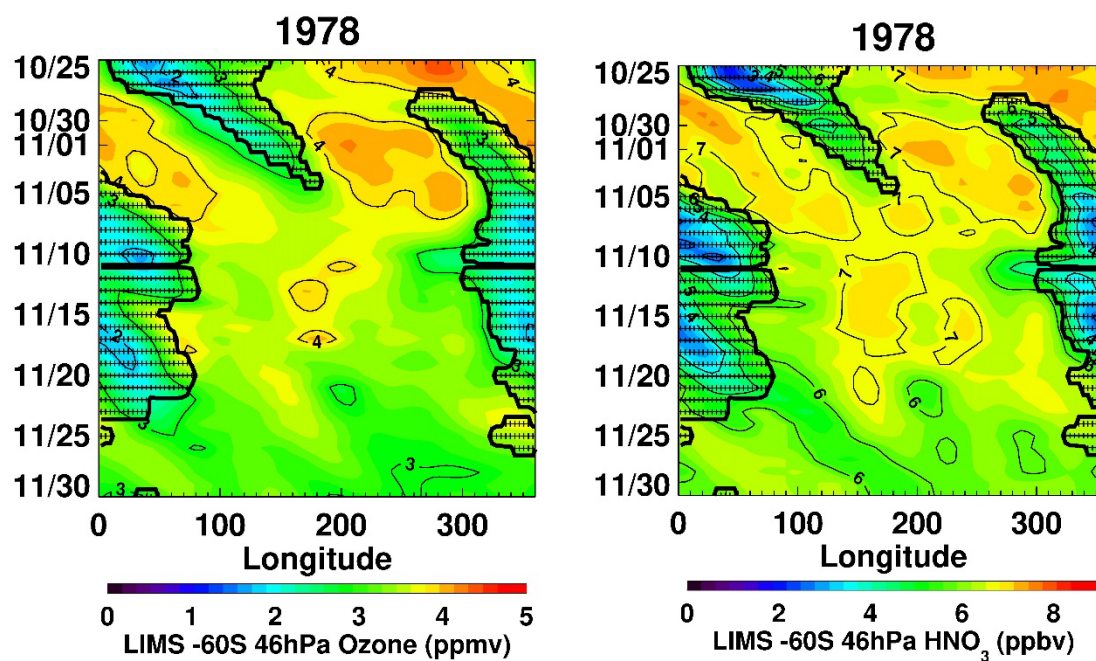


311

312 Figure 5—Time/longitude or Hovmöller plots of LIMS ozone (left) and HNO₃ (right) for 60°S
313 and 46 hPa. The ERA-40 vortex edge shows as thick black contours, and the vortex interior has
314 horizontal dotted lines.

315

316



317

318 Figure 6—As in Fig. 5, but extended in time from October 25 to November 30, 1978.

319